Validating a quasi-linear transport model versus nonlinear simulations

2009 Nucl. Fusion 49 085012

(http://iopscience.iop.org/0029-5515/49/8/085012)

IOP Publishing and International Atomic Energy Agency Nuclear Fusion

Nucl. Fusion **49** (2009) 085012 (10pp) doi:10.1088/0029-5515/49/8/085012

Validating a quasi-linear transport model versus nonlinear simulations

A. Casati[1,a], C. Bourdelle[1], X. Garbet[1], F. Imbeaux[1], J. Candy[2], F. Clairet[1], G. Dif-Pradalier[1], G. Falchetto[1], T. Gerbaud[1], V. Grandgirard[1], Ö.D. Gürcan[3], P. Hennequin[3], J. Kinsey[2], M. Ottaviani[1], R. Sabot[1], Y. Sarazin[1], L. Vermare[3] and R.E. Waltz[2]

[1] CEA, IRFM, F-13108 Saint-Paul-lez-Durance, France
[2] General Atomics, PO Box 85608, San Diego, CA 92186-5608, USA
[3] Laboratoire de Physique des Plasmas, CNRS-École Polytechnique, 91128 Palaiseau Cedex, France

E-mail: alessandro.casati@cea.fr

Received 17 December 2008, accepted for publication 29 May 2009
Published 17 July 2009
Online at stacks.iop.org/NF/49/085012

Abstract
In order to gain reliable predictions on turbulent fluxes in tokamak plasmas, physics based transport models are required. Nonlinear gyrokinetic electromagnetic simulations for all species are still too costly in terms of computing time. On the other hand, interestingly, the quasi-linear approximation seems to retain the relevant physics for fairly reproducing both experimental results and nonlinear gyrokinetic simulations. Quasi-linear fluxes are made of two parts: (1) the quasi-linear response of the transported quantities and (2) the saturated fluctuating electrostatic potential. The first one is shown to follow well nonlinear numerical predictions; the second one is based on both nonlinear simulations and turbulence measurements. The resulting quasi-linear fluxes computed by QuaLiKiz (Bourdelle *et al* 2007 *Phys. Plasmas* **14** 112501) are shown to agree with the nonlinear predictions when varying various dimensionless parameters, such as the temperature gradients, the ion to electron temperature ratio, the dimensionless collisionality, the effective charge and ranging from ion temperature gradient to trapped electron modes turbulence.

PACS numbers: 52.55.Dy, 52.30.Gz, 52.35.Qz, 52.65.Tt

(Some figures in this article are in colour only in the electronic version)

1. Introduction

Rapid but complete physics based transport models are necessary to improve the scenario designing capability of integrated simulation platforms, such as the CRONOS code [1]. After more than 40 years from the first pioneering papers [2, 3], the turbulent fluxes estimations by quasi-linear theory still remain nowadays an open subject of research, that can provide very powerful predictive capabilities. Reviews can be found for example in [4–8]. Even if most of the theoretical efforts have been applied to 1D plasma turbulence, several quasi-linear transport models have been proposed for the tokamak relevant 3D turbulence, providing feasible and commonly used predictive tools, which include GLF23 [9], TGLF [10, 11], IFS-PPPL [12], MMM95 [13], the Weiland model [14] and QuaLiKiz [15]. Despite the apparently crude approximations adopted, the quasi-linear theory has revealed for a relevant number of cases an interestingly good agreement with both experimental results [9, 12] and nonlinear gyrokinetic simulations [10, 11, 16–19].

Validating quasi-linear transport models requires careful study of two distinct points. The first one consists of checking whether the approximation of a linear response for the transported quantities (particles and energy) to the fluctuating potential is realistic or not. The second one deals with the improvement of the arbitrary choices on the saturated electrostatic potential, in terms of the wave-number k and frequency spectra and saturation level. Clarifying these aspects requires intensive comparison with both nonlinear simulations and fluctuation measurements. This is the core of the work presented here.

In section 2, the QuaLiKiz model based on an eigenvalue gyrokinetic code, Kinezero [20] is briefly recalled. The frequency spectrum choice is discussed in the frame of the

[a] Author to whom any correspondence should be addressed.

resonance broadening theory (RBT). The critical choices made for the electrostatic potential k spectra are reviewed in the light of recent comparisons between turbulence measurements, obtained by reflectometry in Tore Supra [21, 22], and nonlinear gyrokinetic simulations, using the Eulerian code GYRO [23] and the semi-Lagrangian code GYSELA [24].

In section 3, the assumption of linear response for the transported quantities to the fluctuating potential is compared with nonlinear simulation results. A Kubo-like number is evaluated in nonlinear simulations. Moreover, overall transport weights are defined and compared in the linear and nonlinear regimes. As in [19], where only pure trapped electron mode (TEM) turbulence has been explored, a good agreement of the de-phasing between the potential and the transported quantities is observed for coupled ion temperature gradient (ITG)–TEM turbulence. On the other hand, contrarily to the observation made in [18] for ETG turbulence, the overall quasi-linear response (which includes both phase and amplitude) is affected by a slight, but constant across many ITG–TEM cases, over prediction with respect to the nonlinear results, as also reported in [25].

In section 4, the total quasi-linear fluxes (combining the quasi-linear response with the choice on the fluctuating potential) given by QuaLikiz are compared with the nonlinear GYRO fluxes, while varying various dimensionless parameters such as the normalized temperature gradient R/L_T, the ion to electron temperature ratio $T_\mathrm{i}/T_\mathrm{e}$, the dimensionless collisionality ν^* and the effective charge Z_eff. One unique coefficient is adopted to renormalize the quasi-linear predictions to the nonlinear fluxes. Interestingly, both the ratios between the transport channels (ion energy, electron energy and particle fluxes) and the parametric behaviour of the fluxes are shown to agree well for coupled ITG–TEM turbulence. Nevertheless, some departures from the nonlinear fluxes are observed for the particle flux and across the TEM to ITG transition at fixed R/L_{T_e}.

In section 5, the results are discussed and a conclusion is drawn.

2. Improved assumptions for QuaLiKiz quasi-linear fluxes

The general approach chosen for this new quasi-linear model QuaLiKiz is briefly recalled. The hypotheses underlying a stochastic quasi-linear theory are reviewed, pointing out the presence of two distinct ways of accounting for broadenings around the resonances. Also, the k wave-number shape of the fluctuating electrostatic potential has been modified in the light of recent comparisons between nonlinear simulations and turbulence measurements.

2.1. The model

The quasi-linear gyrokinetic expression of the turbulent fluxes results from the time average of the nonlinear Vlasov equation over a time τ larger than the largest characteristic time of the transport, $1/\gamma$, where γ is the growth rate, and smaller than the equilibrium evolution time T_0, i.e. in a range where the fluctuating distribution function $\tilde{f}$ is assumed to respond to the fluctuating potentials $\tilde{H}$ through the linearized Vlasov equation. Here, the linearized Vlasov equation is computed by Kinezero using the ballooning representation in the s-α geometry. Kinezero accounts for electrostatic fluctuations only. Two ion species and electrons are taken into account in both their trapped and passing domains. It is an eigenvalue code that computes up to five unstable modes. Collisions on trapped electrons are computed thanks to a Krook operator [26]. For a discussion on the Lorentz versus Krook collision operators see [27].

The quasi-linear formulation leads to the following expressions for the particle and heat fluxes for each species s (respectively Γ_s and Q_s, Q_{Es} being the particle and energy fluxes) [15]:

$$\Gamma_s = \left\langle \tilde{n}_s \frac{ik_\theta \tilde{\phi}}{B} \right\rangle = -\frac{n_s}{R}\left(\frac{q}{r}\right)^2 \frac{1}{B^2} \sum_n \int \frac{\mathrm{d}\omega}{\pi} n^2 \ldots \left\langle \sqrt{\xi} e^{-\xi} \left(\frac{R\nabla n_s}{n_s} + \left(\xi - \frac{3}{2}\right) \frac{R\nabla T_s}{T_s} + \frac{\omega}{n\omega_{Ds}} \right) \times Im\left(\frac{1}{\omega - n\Omega_s(\xi,\lambda) + \mathrm{i}0^+} \right) \right\rangle_{\xi,\lambda} \left| \tilde{\phi}_{n\omega} \right|^2, \quad (1)$$

$$Q_{Es} = \left\langle \frac{3}{2} \tilde{P}_s \frac{\mathrm{i}k_\theta \tilde{\phi}}{B} \right\rangle = -\frac{n_s}{R}\left(\frac{q}{r}\right)^2 \frac{T_s}{B^2} \sum_n \int \frac{\mathrm{d}\omega}{\pi} n^2 \ldots \left\langle \xi^{3/2} \mathrm{e}^{-\xi} \left(\frac{R\nabla n_s}{n_s} + \left(\xi - \frac{3}{2}\right) \frac{R\nabla T_s}{T_s} + \frac{\omega}{n\omega_{\mathrm{D}_s}} \right) \times Im\left(\frac{1}{\omega - n\Omega_s(\xi,\lambda) + \mathrm{i}0^+} \right) \right\rangle_{\xi,\lambda} \left| \tilde{\phi}_{n\omega} \right|^2. \quad (2)$$

In equations (1) and (2), the first summation refers to the discrete toroidal wave-numbers n (where each n labels a poloidal wave-number $k_\theta = nq/r$), while the integration is over the continuous frequency ω. This integration corresponds to the limit passage from a discrete summation over the linear modes labelled by j, i.e. $\sum_j \Rightarrow \int \mathrm{d}\omega$. The spectrum of the saturated potential $|\tilde{\phi}_{n\omega}|^2$ has to be defined in terms of both the dependences on the toroidal wave-number n and the frequency ω. For each n (or k_θ equivalently), the saturated potential can present a ω-spectral structure peaking at different frequencies, corresponding to different unstable modes (in the ion or electron diamagnetic direction). In our model, practically, the integration over the continuous frequency ω is split into a discrete summation over up to five linear unstable modes ($\omega_{kj} + \mathrm{i}\gamma_{kj}$, complex eigenvalues of the linear dispersion relation), retaining for each of them a certain frequency width.

The integrands are $\xi = (\frac{1}{2} m_s V^2)/T_s$, $\lambda = \mu B(r, \theta = 0)/(\frac{1}{2} m_s V^2)$. $b = B(r,\theta)/B(r,0)$, m_s being the mass, V the velocity, μ the adiabatic invariant, B the magnetic field and (r, θ, φ) the radial, poloidal and toroidal coordinates. The frequencies are $n\omega_{\mathrm{D}_s} = -k_\theta(T_s/e_s BR)$, $n\Omega_s = -k_\theta(T_s/e_s BR)\xi(2 - \lambda b) f(\lambda) + k_\parallel V_\parallel$, with $f(\lambda)$ a function of λ depending on the magnetic geometry. n_s is the density, T_s the temperature, P_s the pressure, V_{T_s} the thermal velocity, q the safety factor, s the magnetic shear and α the MHD parameter included in Kinezero, $k_\parallel V_\parallel \approx \pm k_\theta w(s/q)(V_{T_s}/R)\sqrt{\xi}$.

The most delicate part in estimating the turbulent fluxes using quasi-linear theory is due to the fact that the model is not self-consistent (i.e. there is no back-reaction of the perturbed quantities on the fluctuating potential). The linearized gyrokinetic equation does not allow having any information on the saturation of the fluctuating electrostatic potential in terms of its amplitude $|\tilde{\phi}_{n\omega}|$ or on its k and frequency spectral shape. Our choices, detailed here below, are based on the mixing length rule for the saturation level, and on both nonlinear simulations and turbulence measurements for the k and frequency spectra.

Finally, only one global normalization parameter remains to be fixed, in order to renormalize the quasi-linear expectations to the actual nonlinear fluxes predicted by the GYRO nonlinear simulations. This parameter is identical for the particle and energy fluxes. This strategy is quite different from the one chosen in TGLF where three free parameters are chosen to fit at best more than 80 GYRO nonlinear simulations and a fourth parameter is chosen to match one complete ITG–TEM–ETG GYRO simulation. In QuaLiKiz, instead of numerical dataset best fit approach, we test the physical assumptions made at all level of the model, namely the validity of the quasi-linear response, the k and frequency spectra and the saturation level. At the moment, contrarily to TGLF, no $E \times B$ shear stabilization effect is accounted in the present version of QuaLiKiz. Also, the magnetic equilibrium is restricted to s-α in QuaLiKiz, whereas Miller type equilibriums can be retained in TGLF.

2.2. *Resonance broadening and frequency spectra of the fluctuating potential*

In the resonance terms of equations (1) and (2), the finite positive imaginary part $\mathrm{i}0^+$ does not simply fulfil causality; it is also linked to intrinsic nonlinear effects leading to irreversibility through stochastic mixing of the particles orbits in the phase space [8]. In other words, it is the key point for passing from a conventional resonance localized quasi-linear theory to a stochastic quasi-linear theory. Historically, this has been at the origin of the so-called resonance broadening theory (RBT), first initiated by Dupree [28] and followed by several other works, leading also to more elaborate theories, such as the direct interaction approximation (DIA) [29–32]. Hence, in the RBT frame, a non-negligible k dependent imaginary part $\mathrm{i}\nu_k$ is considered. Therefore, in equations (1) and (2), the term $Im(1/\omega - n\Omega_s(\xi,\lambda) + \mathrm{i}\nu_k) = (-\nu_k/(\omega - n\Omega_s(\xi,\lambda))^2 + \nu_k^2)$ is a Lorentzian of width ν_k, in contrast to the singular resonance localized expression found for $\nu_k \to 0$. Also, it is to note that in the limit $\nu_k \to 0$, the particle fluxes are not ambipolar [33], it is hence mandatory to introduce a finite ν_k value.

In principle, two kinds of broadening can exist in the quasi-linear fluxes expressed by equations (1) and (2). The first one actually coincides with the just mentioned RBT. The second one is instead related to an intrinsic ω-spectral shape of the squared fluctuating potential $|\tilde{\phi}_{n\omega}|^2 = |\tilde{\phi}_n|^2 \sum_j S_{nj}(\omega)$ (for each n, there is a summation over j linear unstable modes). Here we refer to this second broadening mechanism as frequency broadening. Assuming, for example, that the frequency spectral shape is described by a function $S_{nj}(\omega)$ centred in ω_{kj} and with a non-zero width α_{kj}, computing the quasi-linear particle flux according to equation (1) should account for both these broadenings, giving

$$\begin{aligned}\Gamma_s &\propto -\sum_n \int \frac{\mathrm{d}\omega}{\pi} n^2 \left\langle Im\left[\frac{\omega - n\omega_s^*}{\omega + \mathrm{i}\nu_k - n\Omega_s}\right]\right\rangle \left|\tilde{\phi}_{n\omega}\right|^2 \\ &= -\sum_{n,j} n^2 \left\langle Im \int_{-\infty}^{+\infty} \frac{\mathrm{d}\omega}{\pi} S_{nj}(\omega) \frac{\omega - n\omega_s^*}{\omega + \mathrm{i}\nu_{kj} - n\Omega_s}\right\rangle \left|\tilde{\phi}_n\right|^2\end{aligned} \tag{3}$$

To our knowledge, most models assume more or less implicitly that for each wave-number k_θ exists a well-defined frequency ω such that $\omega \to \omega_{kj}$. In other words this choice corresponds to

$$S_{nj}(\omega) = \delta\left(\omega - \omega_{kj}\right). \tag{4}$$

In contrast, QuaLiKiz explicitly assumes a Lorentzian shape for the frequency broadening (equation (7) of [15]) in the following way:

$$S_{nj}(\omega) = \frac{-\alpha_{kj}}{\left(\omega - \omega_{kj}\right)^2 + \alpha_{kj}^2}. \tag{5}$$

Interestingly, the QuaLiKiz formulation considering $\nu_{kj} \to 0^+$ coupled to the choice (5) is completely equivalent to the more familiar quasi-linear theory based on RBT where $+\mathrm{i}0^+ = +\mathrm{i}\nu_{kj}$ and $S_{nj}(\omega) = \delta(\omega - \omega_{kj})$. Indeed, starting from the QuaLiKiz choice we obtain

$$\begin{aligned}&\sum_{n,j} n^2 \left\langle Im \int_{-\infty}^{+\infty} \frac{\mathrm{d}\omega}{\pi} \frac{\alpha_{kj}}{\left(\omega - \omega_{kj}\right)^2 + \alpha_{kj}^2} \frac{\omega - n\omega_s^*}{\omega - n\Omega_s + \mathrm{i}0^+}\right\rangle \left|\tilde{\phi}_n\right|^2 \\ &= \ldots - \sum_{n,j} n^2 \left\langle \int_{-\infty}^{+\infty} \frac{\mathrm{d}\omega}{\pi} \frac{\alpha_{kj}}{\left(\omega - \omega_{kj}\right)^2 + \alpha_{kj}^2} \left(\omega - n\omega_s^*\right) \right. \\ &\quad \left. \times \pi\delta\left(\omega - n\Omega_s\right)\right\rangle \left|\tilde{\phi}_n\right|^2 \\ &= \ldots - \sum_{n,j} n^2 \left\langle \frac{\alpha_{kj}}{\left(n\Omega_s - \omega_{kj}\right)^2 + \alpha_{kj}^2} \left(n\Omega_s - n\omega_s^*\right)\right\rangle \left|\tilde{\phi}_n\right|^2 \\ &= \ldots \sum_{n,j} n^2 \left\langle \left(n\Omega_s - n\omega_s^*\right) Im\left(\frac{1}{\omega_{kj} + \mathrm{i}\alpha_{kj} - n\Omega_s}\right)\right\rangle \left|\tilde{\phi}_n\right|^2.\end{aligned} \tag{6}$$

The identity between the frequency broadening proposed in [15] and the RBT is then verified when $\alpha_{kj} = \nu_{kj}$. In other words the QuaLiKiz transport model correctly accounts for both the resonant and non-resonant contributions to the quasi-linear fluxes, as done by the other models such as GLF23, TGLF, the Weiland model, IFS-PPPL and MMM95. Nevertheless, the choices on the shape and the width of this broadening are still arbitrary.

At this point it is important to address the value of such nonlinear resonance broadening ν_k. A rather crude nonlinear dispersion relation is

$$\omega = \omega_k + \mathrm{i}\left(\gamma_k - \nu_k\right). \tag{7}$$

Equation (7) describes a simple dynamics, where for each mode the linear growth rate γ_k competes with the nonlinear

damping ν_k. Within this picture, the saturation is then directly driven from the resonance broadening mechanism when $Im(\omega) \to 0$, i.e. when the nonlinear dissipation balances the linear instability, giving

$$\nu_k = \gamma_k. \tag{8}$$

This is the actual choice in QuaLiKiz. Nevertheless, the frequency width ν_k is equal to the inverse of the auto-correlation time of the fluctuating potential, i.e. $\nu_k = 1/\tau_{ac}$ [8]. Since we are assuming that a nonlinear saturated state is reached, $1/\tau_{ac}$ is expected to be equal or larger than γ_k, hence one would rather expect $\nu_k \geqslant \gamma_k$. Moreover, it is known that even with $\gamma_k = 0$ the nonlinear flux is often non-zero [34]. One way to account for potentially active nonlinear saturation effects (such as non-local couplings in k space) would be to replace $\nu_k = \gamma_k$ by the non-local rule $\nu_k = \gamma_k + k^2 D$; in that way, even if γ_k is zero, $\nu_k = k^2 D$ and stable modes contribute to transport as also suggested by [25].

On the other hand, turbulence measured frequency spectra show that the frequency width scales with k^α with $\alpha \approx 1.2$–1.3 [35, 36], whereas a width proportional to γ would be expected to scale as k. To clarify this crucial point, detailed comparisons between frequency spectra predicted by nonlinear simulations and measured by Doppler reflectometer is presently ongoing on Tore Supra. The result of this study might affect our model. Currently, our model still assumes $\nu_k = \gamma_k$, as done in most existing quasi-linear models.

2.3. Saturation rule of the fluctuating potential

Another critical issue to be addressed by quasi-linear transport modelling is the saturation level of the fluctuating electric potential $|\tilde{\phi}_{n\omega}|$. Following from the former discussion on the quasi-linear assumption of resonance broadening driven saturation (equations (7) and (8)), the level of saturated $|\tilde{\phi}_{n\omega}|$ is linked with the resonance broadening width ν_k.

An estimation of this time scale can be obtained making use of a quite strong hypothesis of random Gaussian statistics for the saturated fluctuating electric field [5], giving

$$\nu_k = \left\langle k_\perp^2 \right\rangle D_\perp. \tag{9}$$

It has to be stressed that the assumption of Gaussian statistics leading to a mixing length rule constitutes a strong additional hypothesis, consistent with a Markovian limit of a diffusion equation. Hence, using the already discussed equality $\nu_k = \gamma_k$ one obtains

$$D_\perp \approx \frac{\gamma_k}{\left\langle k_\perp^2 \right\rangle}. \tag{10}$$

As already mentioned in the previous section, this choice implies that for $\gamma_k = 0$ the flux is also zero, which is known to be false in a number of cases. Hence, any change on the frequency spectrum would as well imply a modification of the actual saturation rule.

In the present version of QuaLiKiz, the saturation level of $|\tilde{\phi}_{n\omega}|^2$ is maximal at $k = k_{\max}$, such that the effective diffusivity D_{eff}, follows the mixing length rule for each unstable mode:

$$\max\left(D_{\text{eff}} \approx \frac{R\Gamma_s}{n_s}\right)\Big|_{k_{\max}} = \frac{R}{n_s}\frac{k_\theta}{B}\frac{n_s e_s}{T_s}\left|\tilde{\phi}_{n\omega}\right|^2\Big|_{k_{\max}} = \frac{\gamma_k}{\left\langle k_\perp^2 \right\rangle}\Big|_{k_{\max}}. \tag{11}$$

The fluxes are a sum over up to five unstable modes. For example, for the particle flux we have

$$\Gamma_s \propto \sum_{n,j} \frac{\gamma_{kj}}{\left\langle k_\perp^2 \right\rangle}\Big|_{k_{\max}} \left\langle \sqrt{\xi} e^{-\xi} \left(\frac{R\nabla n_s}{n_s} + \left(\xi - \frac{3}{2}\right)\frac{R\nabla T_s}{T_s} + \frac{n\Omega_s(\xi,\lambda)}{n\omega_{Ds}} \right) \frac{\gamma_{kj}}{\left(n\Omega_s(\xi,\lambda) - \omega_{kj}\right)^2 + \gamma_{kj}^2} \right\rangle_{\xi,\lambda} \left|\tilde{\phi}_n\right|^2. \tag{12}$$

Each unstable mode is weighted by a saturation rule that uses its corresponding growth rate γ_{kj} and mode structure $\langle k_\perp^2 \rangle$. This is an arguable point; nevertheless, QuaLiKiz fluxes computed in that way are shown to agree well with nonlinear GYRO simulations for mixed ITG–TEM turbulence for a large number of cases, as detailed in section 4. At present, we do not account for the possible stable modes contribution, despite the fact that they might be important as proposed in [25].

The choice for $\langle k_\perp^2 \rangle$ is based on both experimental observations and nonlinear simulation results. It should lead to a maximum $|\tilde{\phi}_{n\omega}|^2$ around $k_\theta \rho_s \approx 0.2$, i.e. lower than the linear stability prediction (typically $k_\theta \rho_s \approx 0.4$), as observed with beam emission spectroscopy (BES) [37] and in nonlinear simulations. It should also depend on q as observed in nonlinear simulations [38, 39]. A pertinent choice for $\langle k_\perp^2 \rangle$ combining these two aspects has been proposed in [16, 38, 40] and recently discussed in [19]. Adding the impact of the MHD parameter α on the curvature drift, one obtains for strongly ballooned modes:

$$\left\langle k_\perp^2 \right\rangle = k_\theta^2 \left(1 + (s - \alpha)^2 \left\langle \theta^2 \right\rangle\right) \tag{13}$$

with

$$\left\langle \theta^2 \right\rangle = \frac{\int \theta^2 \left|\tilde{\phi}_{n\omega}(\theta)\right|^2 d\theta}{\int \left|\tilde{\phi}_{n\omega}(\theta)\right|^2 d\theta}, \tag{14}$$

where $\tilde{\phi}_{n\omega}(\theta)$ is the Gaussian trial eigenfunction used in Kinezero.

2.4. k spectrum of the fluctuating potential

Concerning the k spectral shape of the saturated fluctuating potential, in the previous version of QuaLiKiz we based our choice on turbulence measurements performed by light scattering experiments [41], showing that the density fluctuations $|\tilde{n}_k/n|^2$ wave vector spectrum scales as $e^{-4k\rho_s}$ above $k_\perp \rho_s = 0.5$ and assuming that $|\tilde{n}_k/n|^2 \approx |\tilde{\phi}_k|^2$. In order to increase the confidence in this critical choice, we have compared nonlinear GYRO simulation results with both Doppler and fast-sweeping reflectometry measurements in a Tore Supra ohmic discharge. Nonlinear local gyrokinetic simulations have been performed with GYRO, showing a maximum of the spectrum at $k_{\max}\rho_s \approx 0.2$ down-shifted with respect to the maximum of the linear γ_k spectrum $k_{q,\text{lin-max}}\rho_s \approx 0.4$. A power law of the type $k_\theta \rho_s^{-\alpha}$ is generally able to fit very well both the potential and the density fluctuations spectrum for $k_\theta > k_{\theta,\text{nl-max}}$. A slope $3 < \alpha < 3.5$ has been typically observed (see figure 1), reproducing the experimental turbulence measurements in the medium-low k_θ range from Doppler reflectometry and in k_r from the fast sweeping reflectometry available on Tore Supra [42].

Moreover, recent theoretical work [43] predicts as well a power law decay $\alpha \approx 3$ for scales corresponding to

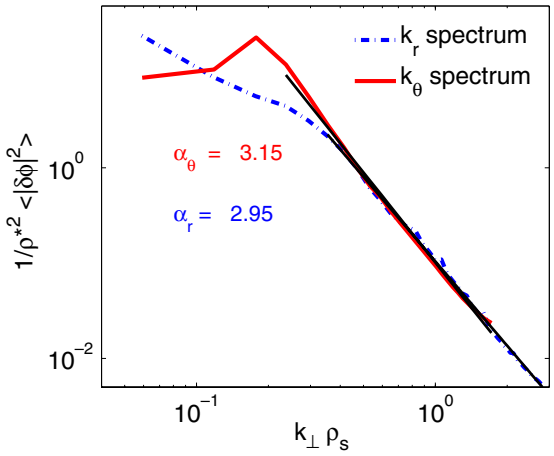

Figure 1. Flux-surface averaged $\delta\phi$ power spectrum in k_r (dotted blue line) and k_θ (continuous red line), computed by the GYRO simulation using parameters from a Tore Supra discharge ($R/a = 3.25$, $r/a = 0.5$, $R/L_{T_i} = 8.0$, $R/L_{T_e} = 6.5$, $R/L_n = 2.5$, $q = 1.48$, $s = 0.72$, $\rho^* = 0.002$, $\nu_{ei}[c_s/a] = 0.0$ and $\beta = 0.0$).

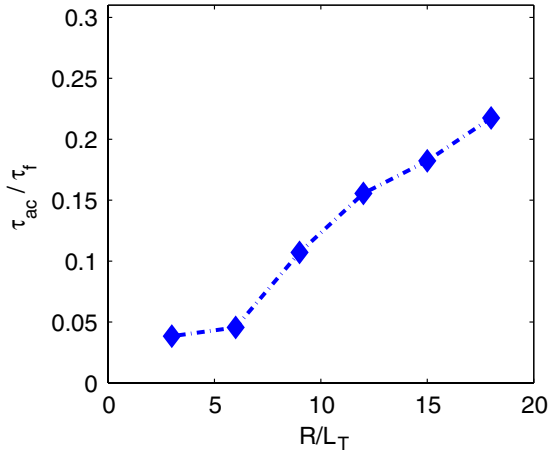

Figure 2. Kubo-like number $K \approx \tau_{ac}/\tau_f$ computed from the GYRO nonlinear simulations versus R/L_T on the GA-standard case.

$k_\perp \rho_s < 1$, and a transition towards $\alpha \approx 6$ for smaller spatial scales ($k_\perp \rho_s > 1$ as observed by the measurements [41]. Nevertheless, these higher k spectral shapes have not yet been investigated in GYRO simulations. Hence, in QuaLiKiz we now assume from 0 to $k_{max}|\tilde{\phi}_n|^2 \propto k_\theta \rho_s^3$ and from k_{max} to infinity $|\tilde{\phi}_n|^2 \propto k_\theta \rho_s^{-3}$.

3. Testing the quasi-linear approximation

3.1. Quasi-linear validity and Kubo number

Historically, the standard quasi-linear theory has been elaborated for test particles [5]. A condition of validity for this quasi-linear framework is that the particles should not be trapped in the field, i.e. the Kubo number K [44] should be lower than one. Nevertheless, there are examples where quasi-linear theory has been shown to work up to $K \sim 1$ [45]. The Kubo number is the ratio between (1) an auto-correlation time τ_{ac} of the fluctuating potential, characterizing the lifetime of the pattern the particle senses and (2) a flight time, τ_f, characterizing the time a particle trapped in the field would interact with the field. Ideally one should compute these two times from nonlinear simulations.

The tokamak turbulence simulations compute the coupled Vlasov–Maxwell equations, hence the definitions of these characteristic times have to be reviewed. τ_f can be calculated as the ratio between an auto-correlation length λ_c, and the velocity at which the fluctuating quantities are radially transported δV_r. In particular, λ_c is a radial correlation decay length, here computed by taking the maximal value along the ridge of the 2D correlation function

$$\langle C(\Delta r, \Delta\varphi)\rangle_{r,\varphi,t} = \frac{\left\langle \tilde{\phi}(r,\varphi)\,\tilde{\phi}(r+\Delta r, \varphi+\Delta\varphi)\right\rangle_{r,\varphi,t}}{\left\langle \left|\tilde{\phi}(r,\varphi)\right|^2\right\rangle_{r,\varphi,t}}$$

at $\theta = 0$ (where r, θ, φ are, respectively, the radial coordinate and the poloidal and toroidal angles), while $\delta V_{r,k} \cong i k_\theta \tilde{\phi}_k / B$. τ_{ac} is the interaction time between the fluctuating transported quantity and the fluctuating field. In our simulations, as done by [18], it can be estimated as $\tau_{ac} = 2\langle D\rangle_{r,\theta,t}/\langle|\delta V_r|^2\rangle_{r,\theta,t}$, where D is the particle diffusivity. In ETG simulations [18], both these times have been calculated, and a low Kubo-like ratio $K \approx \tau_{ac}/\tau_f = 0.1$ have been found coherently with a quasi-linear response.

Here, these characteristic times have been computed from nonlinear GYRO simulations of coupled ITG–TEM turbulence. The adopted parameters refer to the so-called GA-standard case: $R/a = 3.0$, $r/a = 0.5$, $R/L_{T_i} = R/L_{T_e} = 9.0$, $R/L_n = 3.0$, $q = 2.0$, $s = 1.0$, $T_i/T_e = 1.0$, $\rho^* = 0.0025$, $\nu_{ei} = 0.0$ and $\beta = 0.0$. Moreover, no additional $E \times B$ shear coming from an externally imposed radial electric field E_r is considered. If not otherwise specified, all the GYRO simulations presented in this work use the following numerical parameters: box size in the perpendicular directions $[L_x/\rho_s, L_y/\rho_s] = [126, 126]$, radial resolution $\Delta x/\rho_s = 0.75$, 16 complex toroidal modes in the range $0 \leqslant k_y\rho_s \leqslant 0.75$ with 12 grids in the parallel direction, 15 in the gyroaverage and 5 in the radial derivative; there are 128 velocity space grids per spatial cell (8 energies, 8 pitch angles and 2 parallel directions). Real mass ratio $\sqrt{m_i/m_e} = 60$ and drift-kinetic electrons are used. The statistical average values from the nonlinear simulations are typically taken from time averages starting at $100[a/c_s]$ and lasting to $1000[a/c_s]$, where c_s is the ion sound speed. A wide scan on the normalized temperatures gradients $R/L_T = R/L_{T_i} = R/L_{T_e}$ has been explored: the ratio $K \approx \tau_{ac}/\tau_f$ shown in figure 2 exhibit values well below 1.0 even for high gradients. These Kubo-like estimations provide then useful information characterizing the quasi-linearity of nonlinear simulations; the parameters here reported define a region where the quasi-linear models are then expected to succeed in predicting turbulent fluxes, as we will show in the following section.

3.2. Testing the quasi-linear response versus nonlinear simulations

A rigorous validation of the quasi-linear response of the transported quantities to the fluctuating field has to be done apart from any hypothesis on the saturated field. For this purpose, the following transport weight w_k has been defined,

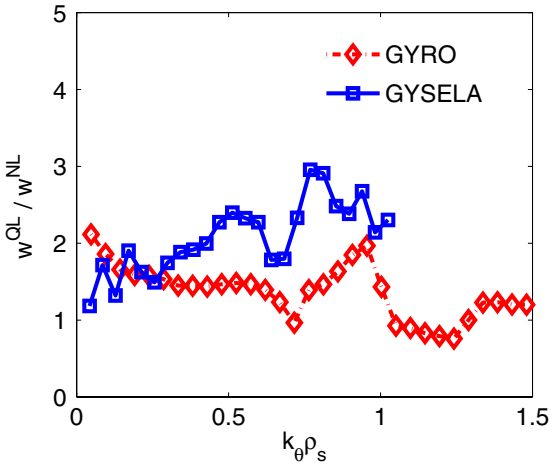

Figure 3. Ratio between the quasi-linear and nonlinear transport weights versus $k_\theta\rho_s$ from local GYRO (red diamonds) and global GYSELA (blue squares) simulations for ITG adiabatic electrons turbulence ($R/a = 2.78$, $r/a = 0.4$, $R/L_{T_i} = 8.28$, $R/L_n = 2.5$, $q = 1.22$, $s = 0.6$, $\rho^* = 0.004$, $\nu_{ei}[c_s/a] = 0.0$ and $\beta = 0.0$).

such that this quantity can be calculated in the full nonlinear as well in the quasi-linear regimes, for each wave-number k and for each transport channel (particle and ion/electron energy). w_k is the ratio between the fluxes at a given poloidal wave-number k_θ (Γ_k, Q_k), divided by the saturated electrostatic potential $|\tilde{\phi}_k|^2$ at a given k. This transport weight is defined as follows:

$$w_k^{\mathrm{NL,QL}} = \left\langle \frac{\langle \Gamma_k\,(r,\theta,t)\,,\, Q_k\,(r,\theta,t)\rangle_{r,\theta}}{\left\langle \left|\tilde{\phi}_k\,(r,\theta,t)\right|^2 \right\rangle_{r,\theta}} \right\rangle_t . \qquad (15)$$

The quasi-linear weights w_k^{QL} can be calculated from an initial value code on the most unstable mode, but in the case of an eigenvalue approach, the fluxes expressed in equations (1) and (2) cannot be unequivocally divided by $|\tilde{\phi}_k|^2$. The discussion on the transport weights is therefore here limited on the linear most unstable mode: a different approach which retains also subdominant modes has been proposed in [33].

The ratio between the quasi-linear and the nonlinear transport weights has been studied by means of both local (GYRO) and global (GYSELA) gyrokinetic simulations of pure ITG turbulence (i.e. with adiabatic electrons). GYSELA simulation has been run with the following numerical resolution [r, θ, φ, $v_\parallel$, μ] = [256, 256, 128, 64, 8] (where θ and φ are the poloidal and toroidal angles, $v_\parallel$ the parallel velocity and μ the adiabatic invariant) on $0.2 < r/a < 0.8$. Figure 3 refers to the k_θ spectral structure of this ratio, where scales up to $k_\theta\rho_s = 1.48$ have been resolved (results corresponding to $k_\theta\rho_s > 1.0$ are omitted for GYSELA since a simplified gyro-averaging operator is applied on these ranges). Both the local and global simulations agree in recognizing a systematic over prediction of the linear transport with respect to the nonlinear regime, with a ratio around 1.5. Moreover, this linear/nonlinear ratio stays reasonably constant when changing the plasma parameters and over the k_θ spectrum, especially at low k_θ scales, where it mostly impacts the transport level [33]. The reason of this over prediction remains to be addressed.

The comparison between the k_θ-structure of the quasi-linear over nonlinear transport weights between GYRO and GYSELA is mainly intended to show that comparable results can be obtained with two different approaches, i.e. performing local δf simulations with GYRO and global full-f simulations with GYSELA. In the following of this work, only the GYRO simulations are used to systematically validate the quasi-linear results against the nonlinear expectations. The principal reasons of this choice are (a) the full-f GYSELA code can be only run for global simulations, resulting in a higher computational cost with respect to the local GYRO runs, (b) nowadays the GYSELA code can operate only with the adiabatic electrons, while the nonlinear expectations on the electron energy and particle transport are essential for the quasi-linear validation.

The comparison between GYRO and GYSELA can be considered quite successful, since most of the turbulent flux is driven for $k_\theta\rho_s < 0.4$. More detailed analysis on the discrepancies at larger scales between the local δf GYRO approach and the global full-f GYSELA one is beyond the scope of this work and it should be addressed in the future. The role of the sheared flows, whose level is different between local and global simulations, can be one of the relevant factors to be explored.

Since the transport weight can be calculated as the real part of a complex quantity, both amplitude and phase can be defined for nonlinear and quasi-linear regimes. Using the initial value code GYRO, the probability density function (PDF) of the de-phasing between the transported quantities (δn, δE_i, δE_e) and the fluctuating potential $\delta\phi^*$ from each k-mode has been calculated in the nonlinear saturation regime and compared with the linear de-phasing from the most unstable mode. Figure 4 shows a very good agreement between the nonlinear and the linear phases in the plane $\theta = 0$, where the interchange instability is supposed to be dominant. This test of validity of the quasi-linear approach, introduced by [19, 38] for pure TEM turbulence, has been in this case successfully extended to coupled ITG–TEM turbulence. Nevertheless, when the plasma parameters are close to the ITG/TEM transition (figures 5(*a*)–(*c*)), the quasi-linear phase coming from the most unstable mode fails on the prediction of particle transport (figure 5(*a*)), whereas very interestingly the linear de-phasing for the energy fluxes remain reasonably close to the nonlinear values (figures 5(*b*) and (*c*)).

4. Parametric impact on quasi-linear fluxes: comparison with nonlinear predictions

In section 2, we have discussed the choices made for the saturated electrostatic potential in the present version of QuaLiKiz, based on nonlinear simulations and experimental measurements. In section 3, we have shown that the major approximation of the quasi-linear theory, namely assuming a linear response for the fluctuating transported quantities, is actually reasonable in a wide number of cases. In this fourth part, we test the whole quasi-linear fluxes computed by the actual version of QuaLiKiz versus nonlinear GYRO simulations for various parameter scans.

Only one renormalization factor, C_0, has been used; this has been chosen to renormalize to the GYRO nonlinear

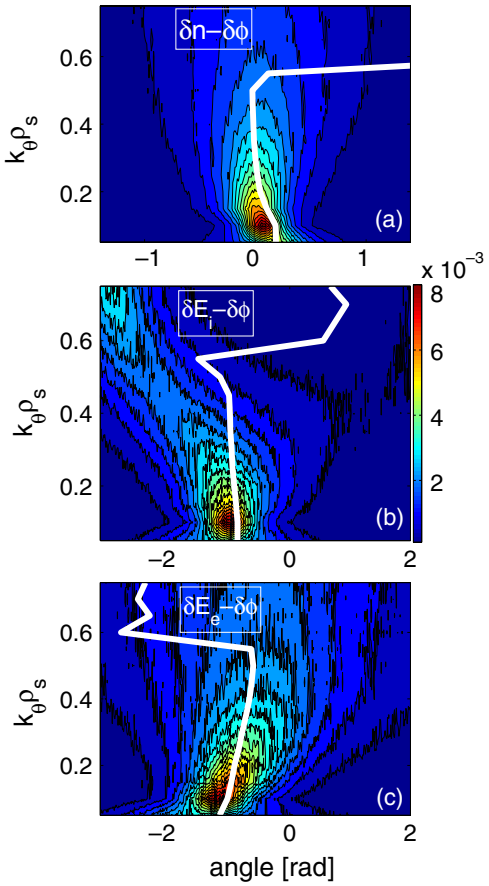

Figure 4. PDF of the nonlinear cross-phases (colour contour plot) and the linear cross-phase on the most unstable mode (white line) between (*a*) δn and $\delta\phi$, (*b*) δE_i and $\delta\phi$, (*c*) δE_e and $\delta\phi$ from the local GYRO simulation on the GA-standard case.

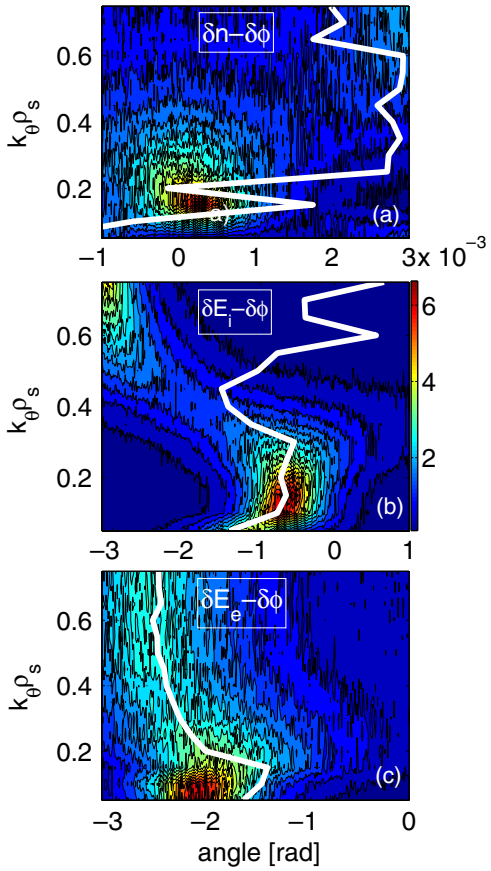

Figure 5. PDF of the nonlinear cross-phases (colour contour plot) and the linear cross-phase on the most unstable mode (white line) between (*a*) δn and $\delta\phi$, (*b*) δE_i and $\delta\phi$, (*c*) δE_e and $\delta\phi$ from the local GYRO simulation on the GA-standard case with modified $R/L_{T_\mathrm{i}} = 6.0$.

prediction the QuaLiKiz estimation of the ion energy flux for the GA-standard case. In the first scan, both the ion and electron temperature gradients are simultaneously varied on a wide range (figure 6). The effective energy and particle diffusivities are defined by the relations $\Gamma_{\mathrm{i,e}} = -D_{\mathrm{i,e}}\nabla_r n_{\mathrm{i,e}}$ and $Q_{\mathrm{i,e}} = -n_{\mathrm{i,e}}\chi_{\mathrm{i,e}}\nabla_r T_{\mathrm{i,e}}$. In this work all the diffusivities are expressed in GyroBohm units $\chi_{\mathrm{GB}} = \rho_s^2 c_s/a$, where $\rho_s = c_s/\Omega_\mathrm{i}$, $c_s = \sqrt{T_\mathrm{e}/m_\mathrm{i}}$ and $\Omega_\mathrm{i} = eB/m_\mathrm{i}$. From $R/L_T = 4.5$ to 13.5, the ion and electron energy and particle fluxes computed by QuaLiKiz and GYRO agree within 15%. Both the ratio between the transport channels and the parametric dependence are well captured by the quasi-linear approach.

The actual hypothesis of the model also imply a fair agreement with the small scale ETG transport predicted by massive ITG–TEM–ETG GYRO nonlinear simulations presented in [34]. With the same core plasma parameters (the GA-standard case with no $E \times B$ shear), the ETG contribution to the total electron energy flux predicted by QuaLiKiz is 11%, in very good agreement with 10% obtained by the GYRO simulation. Nevertheless, this value can be drastically overcome in the presence of additional $E \times B$ shear rates coming from an external radial electric field E_r, which strongly quench the low k ITG–TEM transport, while leaving almost unaffected the ETG contribution, as observed in [11, 34].

A second example is a direct application to an experimental dimensionless collisionality (ν^*) scan realized

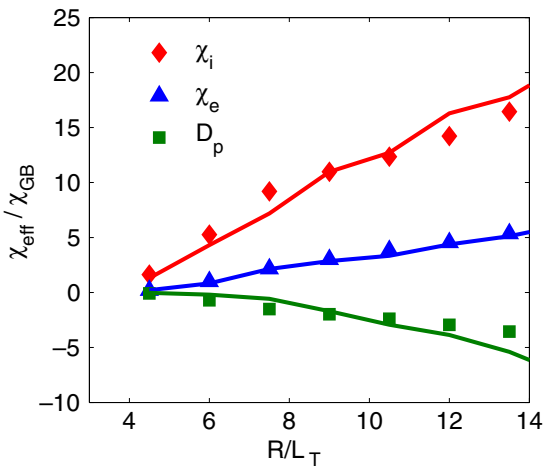

Figure 6. Ion energy, electron energy and particle effective diffusivities from GYRO (points) and QuaLiKiz (lines) for the R/L_T scan based on the GA-standard case.

on Tore Supra plasmas [46]. The ν^* scaling of transport is a crucial test for quasi-linear models. Two effects are potentially at play with opposite consequences on the total flux levels. The collisional damping of sheared flows would in fact result into an increase in the turbulence level at

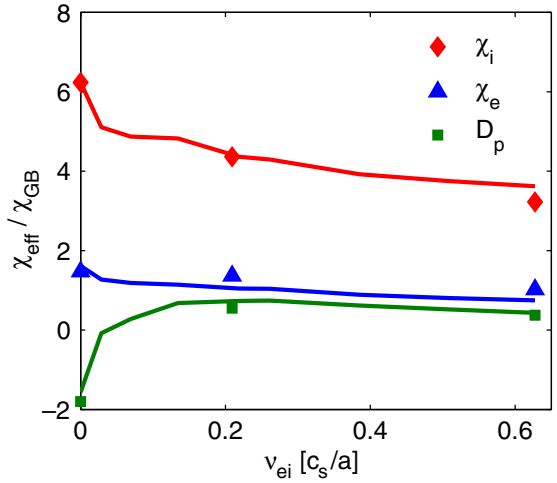

Figure 7. Ion energy, electron energy and particle effective diffusivities from GYRO (points) and QuaLiKiz (lines) for the ν^* scan based on Tore Supra discharges ($R/a = 3.25$, $r/a = 0.5$, $R/L_{T_i} = 8.0$, $R/L_{T_e} = 6.5$, $R/L_n = 2.5$, $q = 1.48$, $s = 0.72$, $\rho^* = 0.002$ and $\beta = 0.0$).

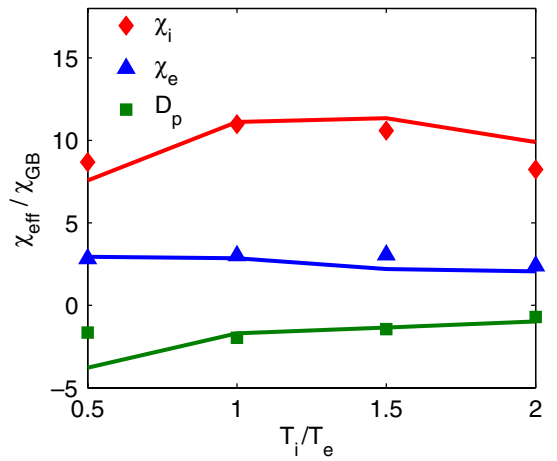

Figure 8. Ion energy, electron energy and particle effective diffusivities from GYRO (points) and QuaLiKiz (lines) for the T_i/T_e scan based on the GA-standard case.

higher collisionality; hence the fluxes would be enhanced. Conversely, the linear collisional TEM damping would act in the opposite direction, reducing the linear instability drive as therefore the total turbulent flux at higher collisionality. For the plasma parameters here explored, the GYRO simulations find a visible reduction in the transport level when increasing the collisionality (figure 7), then the linear TEM damping is found to be dominant in these nonlinear simulations with respect to the collisional drag of sheared flows. Finally, figure 7 demonstrates that, for experimental values of ν^*, the quasi-linear modelling by QuaLiKiz is able to well reproduce the nonlinear diffusivities predicted by GYRO simulations, performed with pitch-angle scattering operators on both electrons and ions. The coupled dynamics between ion and electron non-adiabatic responses is crucial for both GYRO and QuaLiKiz. In particular, the particle flux reverses direction as ν^* increases as expected in [40].

The third scan (figure 8) illustrates a T_i/T_e scan performed on the GA-standard case. Some discrepancy between the

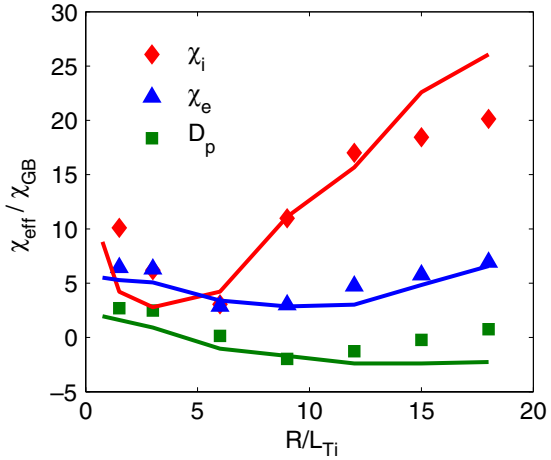

Figure 9. Ion energy, electron energy and particle effective diffusivities from GYRO (points) and QuaLiKiz (lines) for the TEM to ITG transition based on the GA-standard case, fixing $R/L_{T_e} = 9.0$ and varying R/L_{T_i}.

quasi-linear particle flux predicted by QuaLiKiz and the nonlinear result by GYRO is found for $T_i/T_e = 0.5$. This observation is consistent with [33]: the quasi-linear particle flux can in fact break away even by a factor of 2–3 with respect to the nonlinear result for very strongly/weak thermally pinched particle flows. This seems to be one of the most significant quantified failures of quasi-linear modelling.

Figure 9 illustrates the TEM to ITG transition on the GA-standard case, when keeping fixed $R/L_{T_e} = 9$ and varying only R/L_{T_i}. The electron energy fluxes are well matched; discrepancies are instead observed on the particle fluxes for strong ITG turbulence and for the ion energy flux for $R/L_{T_i} < 4$ and $R/L_{T_i} > 13$. At $R/L_{T_i} < 4$, TEMs become the dominant unstable modes, while the marginal conditions for ITG turbulence could be responsible for this quasi-linear failure on the ion energy flux. Additional changes in the saturation rule for dealing with marginality, as done in TGLF, are still to be addressed. On the other hand, above $R/L_{T_i} = 13$, the QuaLiKiz overestimations can be ascribed to a more pronounced effect of zonal flows in the nonlinear saturation of the ion energy transport for ITG dominated turbulence. Hence, the impact of both sheared flows and marginal turbulence on the quasi-linear transport modelling deserves dedicated additional analysis.

Figures 10 and 11 present a dilution scan operated on plasmas with D main ions, electrons and He impurity on the GA-standard case. For both energy and particle transport of all three species, the quasi-linear predictions by QuaLiKiz are shown to rather well agree with GYRO simulations realized with full nonlinear gyrokinetic treatment of the three plasma species.

In conclusion, for these five scans presented here, the parametric dependences given by GYRO nonlinear simulations are qualitatively, and in the most cases also quantitatively, reproduced by the quasi-linear modelling by QuaLiKiz. Some disagreements are indeed reported for the particle fluxes and for ITG marginal conditions. The next level of validation of QuaLiKiz will deal with plasma profiles predictions through integrated transport simulations using the CRONOS code.

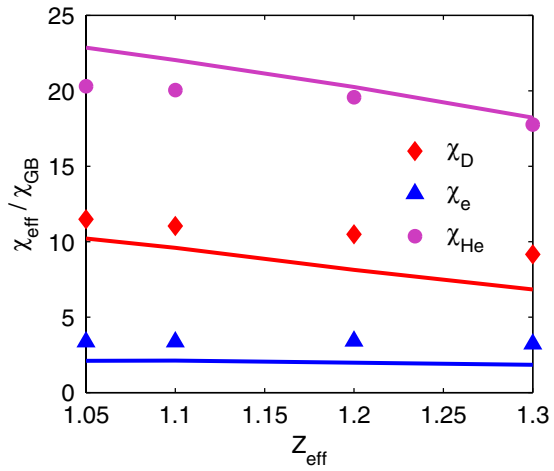

Figure 10. Effective energy diffusivities from GYRO (points) and QuaLiKiz (lines) for a dilution scan, based the on the GA-standard case considering D ions and electrons plasma with He impurity ($T_{\mathrm{He}} = T_{\mathrm{i}}$, $R/L_{T_{\mathrm{He}}} = R/L_{T_{\mathrm{i}}}$ and $R/L_{n_{\mathrm{He}}} = R/L_n$).

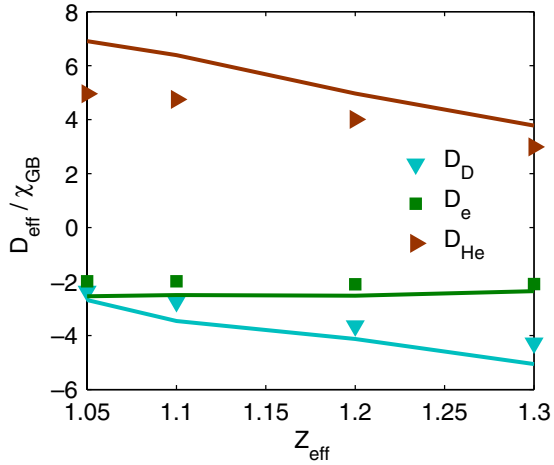

Figure 11. Effective particle diffusivities from GYRO (points) and QuaLiKiz (lines) for a dilution scan, based the on GA-standard case considering D ions and electrons plasma with He impurity ($T_{\mathrm{He}} = T_{\mathrm{i}}$, $R/L_{T_{\mathrm{He}}} = R/L_{T_{\mathrm{i}}}$ and $R/L_{n_{\mathrm{He}}} = R/L_n$).

Further improvements to the actual model will be explored at this point.

5. Discussion

With a unique free parameter, we have shown that the quasi-linear fluxes can reproduce well gyrokinetic nonlinear simulations in a wide range of parameters. The approach followed by QuaLiKiz is based on an accurate comparison between nonlinear simulations and turbulence measurements. Assuming a linear response of the transported quantities to the fluctuating potential has been proven to work rather well for a large number of cases. Moreover, when coupling the choices for the saturated electrostatic potential with the quasi-linear response, we have shown to find quasi-linear fluxes agreeing with nonlinear predictions for energy in the ion and electron channels, as well as for particle fluxes for a wide range of parameters.

Nevertheless, a number of challenging issues remain to be tackled. (i) The choices for the saturated electrostatic potential deserve additional comparisons with nonlinear simulations and experimental measurements. In Tore Supra, both density fluctuations k and frequency spectra by Doppler and fast-sweeping reflectometry are presently under validation against nonlinear simulations. (ii) The way of accounting for subdominant unstable modes in quasi-linear fluxes has to be further deepened. (iii) The domain in which the quasi-linear approach fails (particle flux, marginal conditions, strong ITG turbulence, onset of zonal flows, etc.) should be understood, and compared with the experimental plasma conditions. (iv) Finally, further improvements to the model could be addressed, namely accounting for the $E \times B$ shear stabilization effects and for shaped plasma geometries. In parallel, QuaLiKiz will be coupled to the integrated transport platform CRONOS, allowing to test its predictive capabilities on realistic experimental conditions.

Acknowledgments

A. Casati and C. Bourdelle warmly thank G. Staebler, C. Holland, P. H. Diamond, Z. Lin, F. Jenko and T.S. Hahm for their interest and fruitful interactions.

References

[1] Basiuk V. *et al* 2003 *Nucl. Fusion* **43** 822
[2] Vedenov A.A., Velikov E.P. and Sadgdeev R.Z. 1961 *Nucl. Fusion* **1** 82
[3] Drummond W.E. and Pines D. 1962 *Nucl. Fusion* **3** 1049
[4] Laval G. and Pesme D. 1999 *Plasma Phys. Control. Fusion* **41** A239–46
[5] Krommes J.A. 2001 *Report* PPPL-3546 and http://www.pppl.gov/pub_report
[6] Elskens Y. and Escande D. 2002 *Microscopic Dynamics of Plasmas and Chaos* (Bristol: Institute of Physics Publishing)
[7] Balescu R. 2005 *Aspects of Anomalous Transport in Plasmas* (Bristol: Institute of Physics Publishing)
[8] Diamond P.H., Itoh S. and Itoh K. 2009 *Physical Kinetics of Quasi-Particles in Plasmas* (Cambridge: Cambridge University Press) chapter 3 at press
[9] Waltz R.E., Staebler G.M., Dorland W., Hammett G.W., Kotschenreuther M. and Konings J.A. 1997 *Phys. Plasmas* **4** 2482
[10] Staebler G.M., Kinsey J. and Waltz R.E. 2007 *Phys. Plasmas* **14** 0055909 (APS06 Issue)
[11] Kinsey J., Staebler G.M. and Waltz R.E. 2008 *Phys. Plasmas* **15** 055908
[12] Kotschenreuther M., Dorland W., Beer M.A. and Hammett G.W. 1995 *Phys. Plasmas* **2** 2381
[13] Bateman G., Kritz A.H., Kinsey J.E., Redd A.J. and Weiland J. 1998 *Phys. Plasmas* **5** 1793
[14] Weiland J. 2000 *Collective Modes in Inhomogenous Plasma* (Bristol: Institute of Physics Publishing)
[15] Bourdelle C., Garbet X., Imbeaux F., Casati A., Dubuit N., Guirlet R. and Parisot T. 2007 *Phys. Plasmas* **14** 112501
[16] Jenko F., Dannert T. and Angioni C. 2005 *Plasma Phys. Control. Fusion* **47** B195
[17] Staebler G.M., Kinsey J.E. and Waltz R.E. 2005 *Phys. Plasmas* **12** 102508
[18] Lin Z., Holod I., Chen L., Diamond P.H., Hahm T.S. and Ethier S. 2007 *Phys. Rev. Lett.* **99** 265003
[19] Görler T. and Jenko F. 2008 *Phys. Rev. Lett.* **100** 185002
[20] Bourdelle C., Garbet X., Hoang G.T., Ongena J. and Budny R.V. 2002 *Nucl. Fusion* **42** 892

[21] Gerbaud T. *et al* 2006 *Rev. Sci. Instrum.* **77** 10E928
[22] Hennequin P., Honoré C., Truc A., Quéméneur A., Fenzi-Bonizec C., Bourdelle C., Garbet X., Hoang G.T. and the Tore Supra team 2006 *Nucl. Fusion* **46** S771
[23] Candy J. and Waltz R.E. 2003 *Phys. Rev. Lett.* **91** 045001
[24] Grandgirard V. *et al* 2007 *Plasma Phys. Control. Fusion* **49** B173–182
[25] Hatch D.R., Terry P.W., Nevins W.M. and Dorland W. 2009 *Phys. Plasmas* **16** 022311
[26] Romanelli M., Regnoli G. and Bourdelle C 2007 *Phys. Plasmas* **14** 082305
[27] Fülöp T., Pusztai I. and Helander P. 2008 *Phys. Plasmas* **15** 072308
[28] Dupree T.H. 1966 *Phys. Fluids* **9** 1773
[29] Dupree T.H. 1968 *Phys. Fluids* **11** 2680
[30] Weinstock J. 1969 *Phys. Fluids* **12** 1045
[31] Weinstock J. 1970 *Phys. Fluids* **13** 2308
[32] Orszag S.A. and Kraichnan R.H. 1967 *Phys. Fluids* **10** 1720
[33] Waltz R.E., Casati A. and Staebler G. 2009 Gyrokinetic simulation tests of quasilinear and tracer transport *Phys. Plasmas* submitted
[34] Waltz R.E., Candy J. and Fahey M. 2007 *Phys. Plasmas* **14** 056116
[35] Antar G. *et al* 1999 *Plasma Phys. Control. Fusion* **41** 733
[36] Hennequin P. *et al* 1999 *26th EPS Conf. on Controlled Fusion and Plasma Physics (Maastricht, The Netherlands, 14–18 June)* vol 23J (ECA) pp 977–80 http://epsppd.epfl.ch/Maas/web/pdf/p3006.pdf
[37] McKee G.R. *et al* 2001 *Nucl. Fusion* **41** 1235
[38] Dannert T. and Jenko F. 2005 *Phys. Plasmas* **12** 072309
[39] Hirose A., Livingstone S. and Singh A.K. 2005 *Nucl. Fusion* **45** 1628
[40] Angioni C., Peeters A., Jenko F. and Dannert T. 2005 *Phys. Plasmas* **12** 112310
[41] Hennequin P., Honoré C., Truc A., Quéméneur A., Gervais F., Sabot R. and Fenzi C. 2004 *Plasma Phys. Control. Fusion* **46** B121
[42] Casati A. *et al* 2009 *Phys. Rev. Lett.* **102** 165005
[43] Gürcan Ö.D. *et al* 2009 Dynamics of the wave-number spectrum of drift wave turbulence *Phys. Rev. Lett.* at press
[44] Kubo R. 1963 *J. Math. Phys.* **4** 174
[45] Ottaviani M. 1992 *Europhys. Lett.* **20** 111–6
[46] Gerbaud T. *et al* 2008 *35th EPS Conf. on Controlled Fusion and Plasma Physics (Hersonissos, Crete, Greece, 9–13 June)* http://epsppd.epfl.ch/Hersonissos/pdf/P1_044.pdf